Segregation and diffusion on semiconductor surfaces

J. F. Nützel and G. Abstreiter
Walter-Schottky-Institut, Technische Universität München, Am Coulombwall, D-85748 Garching, Germany
(Received 19 May 1995; revised manuscript received 29 January 1996)

The surface segregation of phosphorus, antimony, and boron in Si molecular-beam epitaxy is investigated experimentally at low temperatures. Rate and temperature dependent measurements are explained by a segregation model, which connects surface segregation with surface diffusion. The model is found to explain quantitatively many available data of segregation on different semiconductor surfaces, explicitly: Si, Ge, and GaAs. [S0163-1829(96)00320-7]

I. INTRODUCTION

In the past two decades the molecular-beam epitaxy (MBE) growth technique has developed rapidly. The possibility to obtain arbitrarily chosen doping and heterostructure layer profiles lead to the invention of different semiconductor devices. The improvement of vacuum technology allows for the growth over a wide temperature range (300–900 °C). Precise and fast change of growth rates over several orders of magnitude (down to 3×10^{-4} nm/s) is possible by electron-beam evaporation sources. Therefore, the growth conditions can be adapted easily to the requirements of the special structures.

The desire for sharper profiles and highly strained metastable layer sequences sets the track for lowering the growth temperatures, especially on Si(001) surfaces. For p-type doping, elemental boron evaporated from high temperature cells has been commonly used within the past few years. This is due to its good incorporation properties. For n-type doping, however, antimony is used despite its bad incorporation properties. At growth temperatures, high enough to obtain good crystal quality, strong segregation occurs. This is explained, up to now, by the so-called two-state model (TSM).[1–4]

The aim of this paper is to compare various systematic experimental results of segregation in dependence of growth rate and temperature and to obtain a quantitative description by a simple model. The paper is organized as follows: First, the experimental setup for sample preparation (Sec. II A) and sample measurement (Sec. II B) is described. The models used up to now are discussed as far as it is necessary to compare them with experiments (Sec. III). In Sec. IV, our experimental results are presented and compared with the predictions of the models and other results. After demonstrating the invalidity of the TSM, a different model is developed in Sec. IV C, on the basis of the experimental results. The surface diffusion model is shown to explain basically all experimental data on group IV surfaces (Sec. IV D). In Sec. IV E, the consequences of this model are discussed.

II. EXPERIMENTAL TECHNIQUES

A. Sample fabrication

The samples were grown in a commercially available SiGe MBE (Riber SIVA 32). Si and Ge are evaporated from electron-beam sources. Flux control is obtained via electron ionization energy spectroscopy, allowing for active control of fluxes down to 3×10^{-4} nm/s. Sb is supplied by a conventional Knudsen effusion cell. Phosphorus is coevaporated together with Si from a sublimation source described elsewhere.[5] The Si flux of the source is calibrated by *in situ* reflection high energy electron diffraction (RHEED) measurements. The P evaporation is calibrated by electrochemical capacitance-voltage (eCV) measurements and secondary ion mass spectroscopy (SIMS) and is found to be very stable and fully electrically active during the whole lifetime of the sublimating Si:P arch, heated by electrical current. The base pressure of the chamber is below the detection limit of 1×10^{-12} torr. The working pressure depends on the heating power of the electron-beam source and is typically at about 10^{-10} torr. Most samples were grown on $n+$ (10 m Ω cm) Si(001) substrates to provide a good back contact for eCV measurements. For boron-doped samples, we used $p+$ substrates. Some samples, which were analyzed only by SIMS measurements of the Sb concentrations were grown on n (1500 Ω cm) substrates. The measured miscut of the substrates is $0.2 \pm 0.05°$. This is very typical for commercially available substrates, intentionally used here. The samples consist of several regions, each grown at constant rate and temperature. We consider it as advantageous to supply the segregating species not as a δ-like layer during a growth interruption. Instead, we supply it continuously during growth maintaining the growth conditions of interest. This is important to secure equilibrium of the surface structure. Otherwise the precise measurement of the decay length might be influenced by transient phenomena observed experimentally[6] and expected theoretically.[7]

B. Sample measurement

The phosphorous doped samples were measured mainly with eCV, using a conventional setup.[8] SIMS reference measurements were performed to verify that the electrical carrier density is equal to the phosphorous atom concentrations. This is described in more detail [full electrical activity, superiority to Sb, successful modeling over the full temperature range (300–900 °C)] elsewhere.[9] The Sb incorporation is measured by SIMS.

For most growth conditions, a second sample with a concentration differing by a factor of 3 was measured to find

0163-1829/96/53(20)/13551(8)/$10.00 © 1996 The American Physical Society

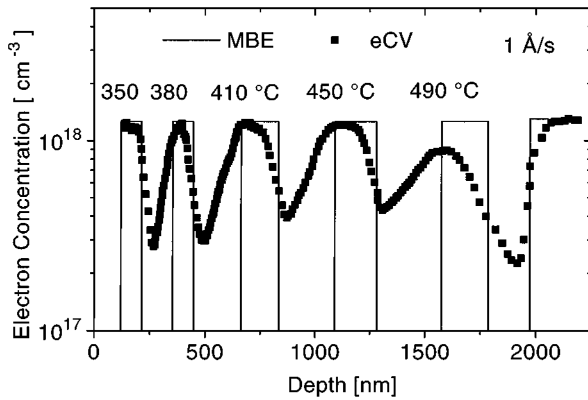

FIG. 1. Typical eCV profile together with the growth proccess data.

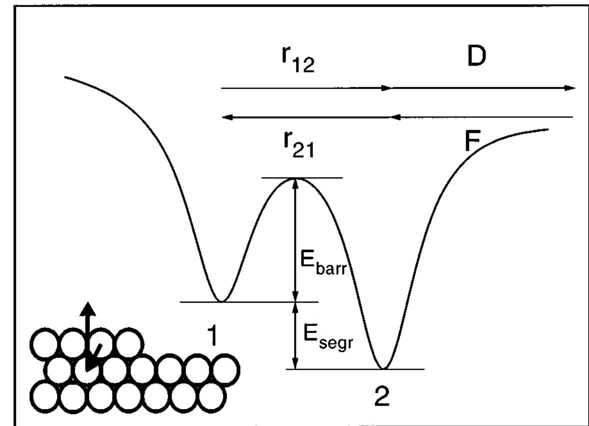

FIG. 2. Two-state model (TSM).

possible deviations from the simple first-order kinetic (higher order kinetic, limited solubility). However, neither noticeable deviations could be found nor significant deviations of the exponential decay. A typical result is shown in Fig. 1. Beginning at the right side, we see first the $n+$ substrate. The leading edge shows a small depletion, which may be due to some residual boron doping at the interface. The boxes indicate the time of dopant supply and the supplied amount. It can be seen that due to the segregation, the incorporated dopant concentrations increases with time. The concentration reaches the supplied concentration asymptotically. For the first box, grown at 490 °C, the thickness of the layer was not enough to reach this equilibrium. After closing the dopant shutter, the concentration decreases simply exponentially. The length required to reduce the concentration to $1/e$ is called the decay or segregation length. Oxygen with an energy of 10 keV was used for the SIMS measurements as an etching ion beam. This results in a measured upper limit for profile broadening of 1.5 nm for the trailing edge. This is in good quantitative agreement with detailed studies on SIMS broadening.[10]

III. MODELS

We describe now the basic features of the most common models for surface segregation. We show their failure to explain many experimental data, which justifies the need for a new one.

A. Adsorption-incorporation-desorption model

This first model was introduced to explain transient effects and small incorporation/sticking coefficients of atoms observed on Si at higher temperatures[11] in a phenomenological way. In a more general form, combining[12,13]

$$\frac{dN_{DS}}{dt}=F_D-\sum_p K_{Dp}(N_{DS})^p-\sum_q K_{Iq}(N_{DS})^q. \qquad (1)$$

N_{DS} is the surface concentration, F_D the incoming (dopant) flux, and the K's are the coefficients of the desorption (D) and incorporation (I) processes with the orders p and q. For most experimental situations only the first-order coefficients ($p,q=1$) were found to be important. Observations of higher order processes for desorption were later decomposed again to simple first-order kinetic from Sb on Si and Sb on Sb terminated Si surface with a desorption energy very similar to pure Sb (Ref. 14). The coefficients K_{Dp}, K_{Iq} were determined experimentally. At higher temperatures most of them were found to have an Arrhenius-like temperature dependence.[11]

The incorporation probability $p_{\rm inc}[=K_{I1}/\text{Rate (ML/s)}]$ is determined by the decay length of the simple exponentially decaying concentration in the layers grown without additional supply of the segregating species. As long as simple first-order kinetics is relevant, which means that the surface concentration is much less than 1 ML, and that desorption, bulk diffusion, and other processes are negligible, the relation between incorporation probability $p_{\rm inc}$ and the decay length Δ is simply given by

$$p_{\rm inc}=\frac{a_0}{4\Delta}, \qquad (2)$$

with the thickness of 1 ML = $a_0/4=1.358$ Å for Si(001).

Observations of nonexponential decays[13] at high coverages of the second atom species were interpreted with the introduction of second-order coefficients. To our knowledge, growth rate dependencies were never taken into account in modeling, although appropriate measurements have been done [e.g., for Ge on Si (Ref. 13)]. In summary the adsorption-incorporation-desorption (AID) model sets up the formal frame to describe the time evolution of the surface concentration, resulting in the depth distribution of the segregant. The AID needs, as a parametrization, the incorporation coefficients, derived from microscopic models.

B. Two-state model

The often observed reversal of segregation,[2,3] to lower segregation lengths at lower temperatures, made the so-called two-state model popular. The two-state model is a rather intuitive approach, which describes segregation as a two particle exchange process between the surface layer and the next layer beneath, which can happen at any surface position (Fig. 2). For the low temperatures relevant, we can neglect desorption. This model evolves from considering volume/surface segregation through bulk diffusion for metal alloys,[1] including self-limitation, several bulk layers. The

test frequency was found to be in agreement with the expectation from equipartition theorem (e.g., Ref. 15):

$$\nu_{\text{test}}=\frac{k_B T}{h}, \tag{3}$$

with T the growth temperature. A second possibility to obtain a rough estimate of the test frequency is derived from the Debye temperature (e.g., Ref. 16):

$$\nu_D=\frac{k_B \Theta_D}{h}, \tag{4}$$

which gives obviously very similar numbers ($\Theta_{D,\text{Si}}$ = 635 K). The TSM was applied to Sn segregation on GaAs,[2] however, with some limitations discussed in Sec. IV D. It was then adopted to Sb on Si.[3,4] Self-limitation effects in this model were pointed out for Ge on Si in Ref. 17. Due to the simplicity of the model four parameters are sufficient, namely, two activation barrier energies and two test frequencies for the exchanges up and downwards. It was never tried, to our knowledge, to determine the frequencies (on Si). So both frequencies are repeatedly taken as the same and fixed at an arbitrarily taken value in the $10^{12}-10^{13}$ s^{-1} range.

The rate equations are

$$\frac{dc_1}{dt}=-c_1(1-c_2)r_{12}+c_2(1-c_1)r_{21}, \tag{5}$$

$$\frac{dc_2}{dt}=c_1(1-c_2)r_{12}-c_2(1-c_1)r_{21}, \tag{6}$$

$$r_{12}=\nu_1 \exp\left(-\frac{E_1}{k_B T}\right), \tag{7}$$

$$r_{21}=\nu_2 \exp\left(-\frac{E_2}{k_B T}\right), \tag{8}$$

with the concentrations c_1, c_2 of the segregating species in the layers 1 and 2 as specified in Fig. 2 normalized to the sheet density of 1 ML (=6.78 × 10^{14} cm^{-2}) and ΔE the difference of the activation energies $E_1=E_{\text{barr}}$ and $E_2=E_{\text{barr}}+E_{\text{segr}}$.

In Fig. 3, the behavior of the TSM and the aperiodic model, described later, is illustrated for the parameters E_{barr}=1.76 eV, $\nu\tau$=2 × 10^{11}, and ΔE = 1.23 eV. The model has two asymptotic regimes: thermal equilibrium at high temperatures and the kinetic limit at low temperatures. In the first case, so many exchanges take place during the growth of one monolayer, that the concentrations are simply given by

$$\frac{c_1}{1-c_1}=\frac{c_2}{1-c_2}\frac{\nu_2}{\nu_1}\exp\left(-\frac{\Delta E}{k_B T}\right). \tag{9}$$

For small concentrations ($c_1, c_2 \ll 1$), the derived segregation length Δ reduces to the well-known equilibrium equation:

$$\Delta_{\text{equil}}=\frac{a_0}{4}\frac{\nu_2}{\nu_1}\exp\left(\frac{E_{\text{segr}}}{k_B T}\right), \tag{10}$$

with $a_0/4$ the thickness of 1 ML. From data in this region, one can determine the segregation energy independent from

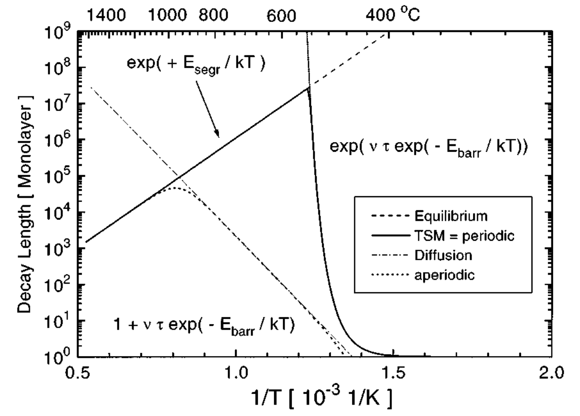

FIG. 3. Principal dependence of segregation lengths for the two-state model (= periodic stepwise) and the aperiodic model vs growth temperature.

the barrier energy and the absolute test frequencies. Neglecting differences of the frequencies the segregation energy can be determined, in principle, by only one experimental point. The experimental values on Si(001) are for Sb: E_{segr}= 1.2 eV;[18] and for Ge: E_{segr}= 0.28 eV.[17]

In the second kinetically limited case, the hopping rate downward is negligible and the segregation length reduces to[3]

$$\Delta_{\text{TSM}}=\frac{a_0}{4}\times\exp\left[\frac{\nu a_0}{4R}\exp\left(\frac{-E_{\text{barr}}}{k_B T}\right)\right], \tag{11}$$

with the decay length Δ, the growth rate R, temperature T, the barrier energy E_{barr}, and ν the test frequency. Fixing the frequency, which was done arbitrarily in different publications, allows the calculation of the barrier energy from the measured decay length [Sb: 1.78 eV (Ref. 4), with $\nu=2\times10^{12}$ s^{-1} or 1.8 eV, with $\nu=3\times10^{13}$ s^{-1};[19] Ge: 1.63 eV (Ref. 17)].

Later published data by Jorke *et al.*[20] for Sb show significant segregation at lower temperatures remarkably deviating from the expected dependence in the low temperature region (< 350 °C). Nakagawa and co-workers[21,22] found also strong segregation for both Sb and Ga on Si(001)

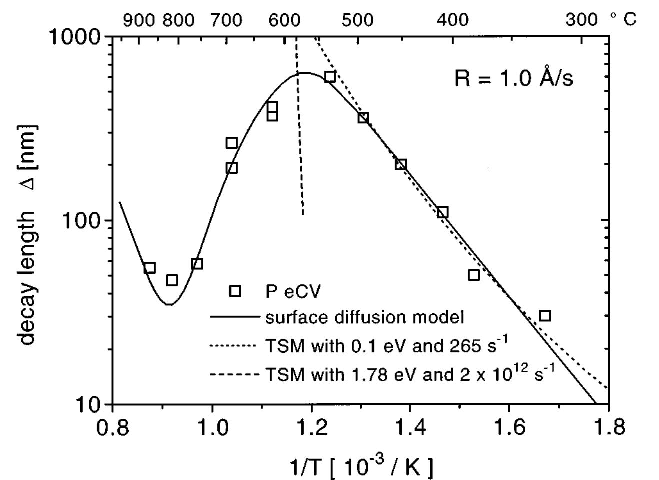

FIG. 4. Segregation lengths of phosphorous vs growth temperature.

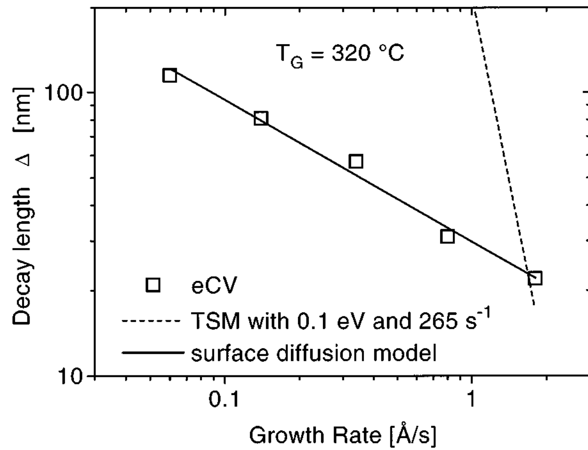

FIG. 5. Segregation length of phosphorus vs growth rate.

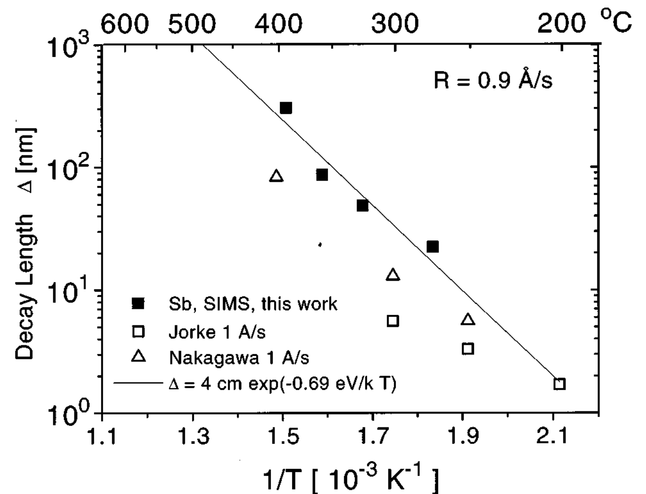

FIG. 6. Segregation lengths of antimony vs growth temperature.

and Si(111), even down to room temperature. The described model is up to now widely accepted[23] and attracted more attention compared to former models[11,21,24] focusing on the order of the incorporation kinetics.

C. Aperiodic Aziz model

The models of Aziz,[25,26] which describe the segregation at solid/liquid interfaces during resolidification, were adopted to MBE by Tsao.[27] The continious growth model with periodic step flow takes the same physcial mechanism into account, namely, an energy difference for the dopant for bulk and surface states and a diffusion exchange beyond an energy barrier between the two states. The resulting dependence reproduces, therefore, the Jorke curves with a slight modification at the crossover between high temperature equilibrium and the low temperature kinetic limit.

For the aperiodic model, Tsao wrote[27]

$$p_{\mathrm{inc}}=\frac{\exp\left(\frac{-E_{\mathrm{segr}}}{k_B T}\right)+(\nu\tau)^{-1}\exp\left(\frac{+E_{\mathrm{barr}}}{k_B T}\right)}{1+(\nu\tau)^{-1}\exp\left(\frac{+E_{\mathrm{barr}}}{k_B T}\right)}, \qquad (12)$$

with ΔE the energy difference between surface and bulk state for the dopant, ν is the test frequency for the diffusion from the subsurface into the surface atomic layer, τ the time to grow 1 ML, and E_{barr} the activation barrier energy for the diffusion. This model reproduces again, at high temperature, the well-known Arrhenius-type behavior. At lower temperatures, shown in Fig. 3, the resulting decay length is $\Delta=(\nu\tau)\exp(-E_{\mathrm{barr}}/k_B T)$.

IV. RESULTS AND DISCUSSION

A. Experimental results

The decay lengths of P on Si(001) were measured for different growth temperatures and rates. The following results are derived from measurements like the one shown in Fig. 1. The temperature dependence of the phosphorous segregation is shown in Fig. 5 over the full temperature range, although we want to focus only on the low temperature part. The segregation behavior at higher temperature ($>$ 600°C) is well understood for both P (Ref. 9) and Sb, taking the mechanisms' equilibrium segregation, desorption, and bulk diffusion at very high temperatures into account. These mechanisms were already studied extensively for other doping species.[11,28,29,24]

In this paper, we focus on the behavior at low temperatures, which are necessary to achieve high incorporation. To shed more light on the segregation mechanism, we performed also rate dependent measurements (Fig. 6). As can be seen from Fig. 6, the rate dependence of the segregation length is rather weak and can be ascribed as a simple inverse square root dependence. To exclude first, that this behavior may be a speciality of P on Si(001), and second, that simplicity of the observed behavior is to be due to some luckily chosen growth parameters, we performed additional measurements with Sb on Si(001) using SIMS. The temperature dependent and rate dependent results are shown in (Figs. 4 and 7). The results reveal a very similar dependency, however with segregation lengths approximately by a factor of five higher. The differences of the absolute values for Sb decay lengths compared to results of other groups may be due to uncertainties in temperature determination, while the

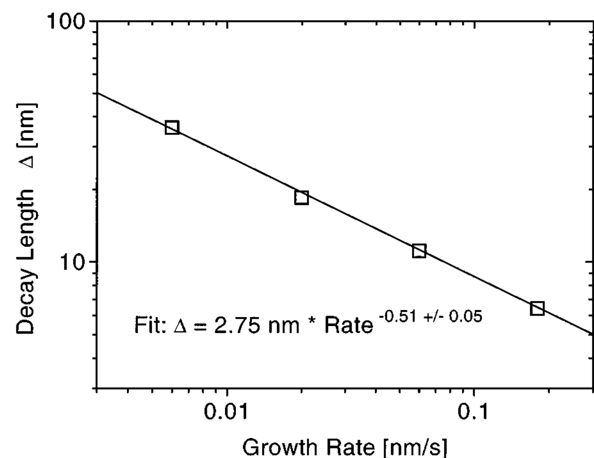

FIG. 7. Segregation lengths of antimony vs growth rate.

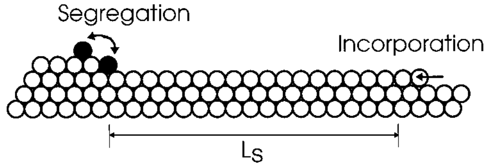

FIG. 8. Surface diffusion model (SDM).

activation energies, derived from the slopes, of 0.5 (Ref. 21)–0.75 eV (Ref. 13) are however very similar.

B. Comparison of models and experiments

In the kinetically limited regime at low temperatures, the segregation lengths determined experimentally show a smooth simple exponential behavior vs 1/T. This differs strongly from the expectations of the two-state model. For reasonable values of ν the temperature dependence should be much steeper. If we nevertheless try to make a least-square fit with the TSM, to determine first the barrier energy and then the test frequency, we obtain the completely unrealistic values $E_{\rm barr}$ = 0.10 eV and ν = 255 s^{-1}. Furthermore, the rate dependence of the decay length has to be

$$\frac{\partial(\ln\Delta_{\rm TSM})}{\partial(\ln R)}=-\ln\left(\frac{4\Delta}{a_0}\right)\ll-1. \tag{13}$$

In contrast, the experimental results for P on Si(001) (Fig. 6) give

$$\frac{\partial(\ln\Delta_{\rm exp})}{\partial(\ln R)}=-0.50\pm0.10. \tag{14}$$

This result cannot be fitted within the two-state model with any set of parameters. From these observations, we conclude the invalidity of the two-state model for this low temperature segregation on silicon.

The aperiodic Aziz model is much nearer to the experimentally observed behavior. Nevertheless, the argument of very low parameters for the barrier energy (0.66 eV) and the frequence ($\approx 6\times10^7$ s^{-1}) remains valid. Additionally the rate dependence of the aperiodic Aziz model is linear, in contrast to the experimental square root behavior. From this we conclude that the adaption of Aziz's model for resolidification, made by Tsao, does not help to explain the observations.

C. Surface diffusion model

We want to demonstrate now, that the experimental results can be explained consistently, taking surface diffusion and steps into account. In this model, segregation takes place as step hopping. The segregant is incorporated only if it is blocked at a step place by an additional atom (see Fig. 8). The step density is controlled by surface diffusion. To keep the formulas as simple as possible, the model is developed for a simple cubic lattice. For the diamond lattice, the prefactor turns out to be the same.

Limited surface diffusion plays an important role at low growth temperatures used for high incorporation. For these growth conditions, RHEED oscillations occur,[30] indicating that growth does not proceed via step flow to steps given by the miscut.

We define an effective surface diffusion constant,

$$D^*=D_0\exp\left(\frac{-E_1}{k_BT}\right). \tag{15}$$

During growth, an average equilibrium step density will develop with an average step size of

$$L_S=\sqrt{D^*(T)\tau}, \tag{16}$$

with $\tau=a_0/4R$ the time required to grow 1 ML. R is the growth rate. The probability that a certain lattice point is a step position becomes

$$p_{\rm step}=\frac{a_0}{L_S}. \tag{17}$$

For growth conditions, for which at least a few surface diffusion events happen for every atom, before it is incorporated, an equilibrium is achieved for the segregant to sit on a step (with concentration $c_{\rm step}$) and plain surface sites ($c_{\rm avg}$), resulting in

$$c_{\rm step}=c_{\rm avg}\exp\left(-\frac{\Delta E}{k_BT}\right). \tag{18}$$

ΔE is the energy difference in thermal equilibrium for the segregant sitting on the different places. The segregating species is only incorporated, if it is at a step site when another atom is adjoining.

$$p_{\rm inc}=\frac{c_{\rm step}}{c_{\rm avg}}p_{\rm step}=\frac{a_0}{L_S(T,R)}\exp\left(-\frac{\Delta E}{k_BT}\right). \tag{19}$$

This can be transformed with Eqs. (2), (16) to

$$\Delta_{\rm kin}=\sqrt{\frac{\nu a_0^3}{4R}}\exp\left(\frac{-E_s}{k_BT}\right). \tag{20}$$

We can rewrite Eq. (20) by normalizing the growth rate to a suitable value R_0,

$$\Delta_{\rm kin}=\Delta_0\sqrt{\frac{R_0}{R}}\exp\left(\frac{-E_s}{k_BT}\right), \tag{21}$$

with Δ_0 and $E_s=E_1/2-\Delta E$ taken here as experimentally determined values. The remaining **two** parameters are determined by experiment [for P on Si(001): Δ_0 = 8 mm, with R_0 fixed at 1 Å/s corresponding to $\nu=1.6\times10^{14}$ s^{-1} and E_s= 0.66 eV]. Both values are well within the reasonable range. For Sb we obtain nearly the same energy (0.69 eV), but decay lengths about five times higher (4 cm).

D. Comparison with other material combinations

In this section, we want to apply the segregation model to explain data of other material combinations. This is in order to see limitations of the model. We demonstrate that this behavior is not specific to the examples studied here, but rather general. In Fig. 9 we compare our data for B doping in Si with other published data.[31] The segregation lengths were

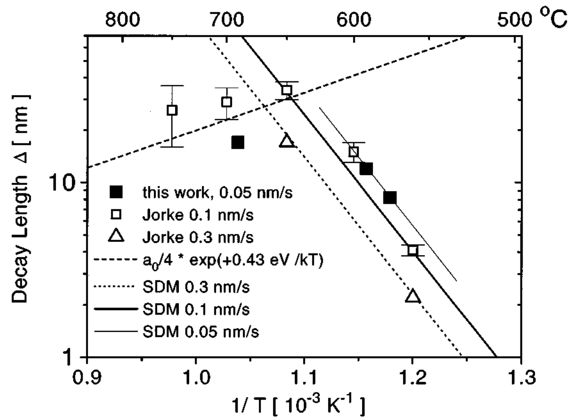

FIG. 9. Segregation lengths of boron vs growth temperature and rate.

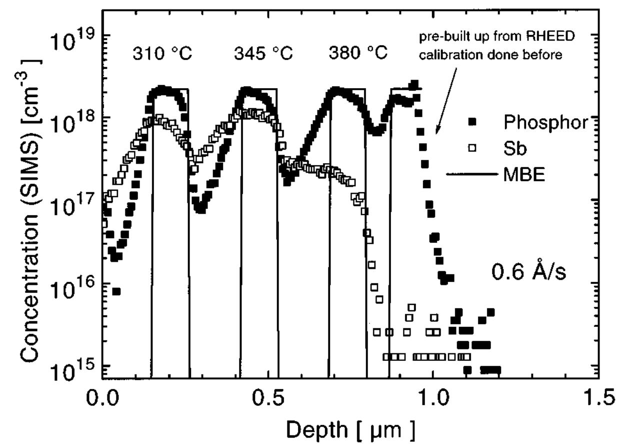

FIG. 10. Direct comparison of P and Sb segregation on Si(001) for different growth temperatures.

found to be much smaller compared to the n-dopants Sb and P. Very similar to P is the existence of a high temperature equilibrium segregation regime with a segregation energy of 0.43 eV. A fit of the TSM results again in a very low energy of about 0.3 eV and a frequency of about 3000/s. The rate dependence reproduces nicely the square root prediction of the surface diffusion model and is in strong conflict with the TSM. The transition to the equilibrium segregation regime happens approximately at the temperature of the crossover to step flow growth expected from STM pictures. However, the fitted frequency is rather high. This may be explained by selective hopping of the boron for different step configurations. A similar behavior is observed for the segregation of P on silicon-germanium surfaces.[32]

The second test is the segregation of Sb on Ge(001). The obtained segregation lengths of Wilhelm *et al.*[33] reproduce also the simple exponential behavior predicted by the SDM. The precise determination of the frequency is however difficult, due to the special growth/measurement sequence applied there. Nevertheless the ranging above 10^{10} s^{-1} is very reasonable. Also an energy of 0.3 eV, significantly lower than the values on Si, is consistent. Again attempts to fit the TSM dependencies results in extremely low energies and frequencies and strong differences between the observed values and the fitting curve. Sn on Ge(001) behaves very similar.[34]

The third test is the segregation of Ge on Si(001). This was first observed by Eberl *et al.*[35] with AES. Recently, data were obtained by Godbey *et al.* with x-ray photoemission spectroscopy (XPS) (Ref. 36) over the full temperature range. The data of XPS intensities, due to the residual Ge concentration at the surface after overgrowth of 10 nm Si, are converted to decay lengths. The conversion procedure is very similar to calculations applied by the authors themselves earlier[37] and includes self-limitation. If we make a fit to the TSM, we get rather unrealistic values of 170 s^{-1} for frequency and 0.1 eV for the energy. Fitting the data with the SDM (below 350 °C), we achieve reasonable values of 0.66 eV and 1.5 mm. The latter can be transformed to a frequency of 5.6×10^{12} s^{-1}.

We are coming back to the paper of Harris *et al.*,[2] who studied Sn segregation on GaAs, where the TSM was adopted first to semiconductors. They state clearly that the frequency is about 5000 s^{-1} and the barrier energy about 0.5 eV. Therefore, the argument that these values are very low and completely different to theoretical expectations of Debye frequency or equipartition theorem holds again. Additionally, the observed rate dependence is much closer to the prediction of the SDM. Similar arguments hold for a segregation study of $In_xGa_{1-x}As$/GaAs (Ref. 38) (the only one, to our knowledge, on III/V surfaces, which allows for quantitative interpretation), and for Sb and Ga segregation on Si(111).[22]

To summarize this section, we found good agreement with the surface diffusion model for all material combinations, for which reliable data are available, and strong conflicts with the two-state model. Especially all rate dependent measurements, that we know about, support strongly the diffusion model. From this we conclude that this type of segregation is a general property of semiconductor surfaces.

After demonstrating the predictive power of the surface diffusion model beyond the simple and accurate description of temperature and rate dependence of P and Sb segregation, we consider additional consequences of the model. If we compare the low temperature energies E_S, for P, Sb, and Ge on Si(100) in Table I, we find very similar values for these three segregants. This might raise the question of whether the small differences are only due to experimental differences or due to dopant induced surface changes. We have performed a direct comparison of P and Sb, supplying both in the same MBE machine at the same time, and measured the incorporation with SIMS (Fig. 10). First we see clearly, that the phosphorous has significant lower decay lengths. Second, we can exclude, that the difference between P and Sb are due to Sb induced surface changes, because these

TABLE I. Segregation energies and lengths (for R=0.1 nm/s) on Si(001).

Segregant	E_{equil} (eV)	E_s (eV)	Δ cm
P	0.64	0.66	0.8
Sb		0.69	4
B	0.43	1.55	960
Ge	0.24	0.66	0.15

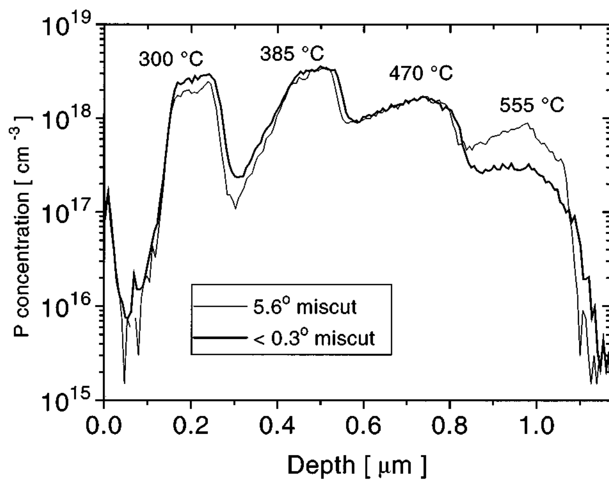

FIG. 11. Segregation of phosphorus on Si(001) in dependence of growth temperature and miscut angle.

changes should influence the P segregation in the same way. We conclude, that it is the step-climbing part in the segregation process, which is dependent on the specific element.

E. Influence of the miscut angle

The next difference is the influence of the miscut of the substrates makes an important difference for the different segregation models. For the TSM, we do not expect significant difference, as long as the percentage of step sites is small, which may have a different two particle exchange dynamic. For the SDM however, we would expect differences if the length of the vicinal step becomes shorter than the length evolving from the surface diffusion dynamic. The experimentally observed crossover points for small concentrations from the low temperature surface diffusion limited segregation described in this paper to the high temperature equilibrium segregation [P on Si(001), 0.1 nm/s, miscut 0.2 °: 580 °C Fig. 5; B on Si(001), 0.1 nm/s, miscut unknown, but assumed to be small: 650 °C Fig. 9] are in good agreement with STM observations of this transition [Si on Si(001) 0.0027 nm/s, miscut 0.3 °, $<$500 °C (Ref. 39)]. This would allow us to interpret also the high temperature equilibrium segregation to act via surface diffusion and not via a two particle exchange. This results in a significant reduction of segregation on substrates with higher miscut at higher temperatures. This is indeed what we observe, as can be seen in Fig. 11. In this figure, the phosphorous concentration is shown for identical growth sequences on a wafer with a high miscut angle of 5.6 °, in comparison with a substrate nominally without miscut. For the temperatures below 500 °C, there is no difference between the segregation behavior. For the highest temperature (555 °C), however, we see a clearly increased incorporation for the miscut substrate.

V. CONCLUSION

We have measured with SIMS and eCV the low temperature segregation lengths of both P and Sb on Si(001) in dependency of both growth temperature and rate. A model is developed, which accurately describes the observed dependencies. The surface diffusion model links surface segregation strongly to surface diffusion. The model is able to describe many data on segregation on semiconductors in a better way than previous models, especially concerning rate dependencies.

ACKNOWLEDGMENTS

Part of this work was supported financially by the SIEMENS AG, Munich via Sonderforschungseinheit. SIMS measurements were performed by Dr. Jahnel and Fr. Lange-Gieseler from Siemens, Neuperlach.

[1] S. Hofmann and J. Erlewein, Surf. Sci. **77**, 591 (1978).
[2] J.J. Harris, D.E. Ashenford, C.T. Foxon, P.J. Dobson, and B.A. Joyce, Appl. Phys. A **33**, 87 (1984).
[3] H. Jorke, Surf. Sci. **193**, 569 (1988).
[4] H. Jorke, H.-J. Herzog, and H. Kibbel, Phys. Rev. B **40**, 2005 (1989).
[5] E. Friess, J.F. Nützel, and G. Abstreiter, Appl. Phys. Lett. **60**, 2237 (1992).
[6] J.F. Nützel and E. Friess (unpublished).
[7] M. Kardar, G. Parisi, and Y. Zhang, Phys. Rev. Lett. **56**, 889 (1986).
[8] BIORAD, Polaron PN4200 Etchprofiler, Munich, 1981.
[9] J.F. Nützel and G. Abstreiter, J. Appl. Phys. **78**, 937 (1995).
[10] M.G. Dowsett, R.D. Barlow, H.S. Fox, R.A.A. Kubiak, and R. Collins, J. Vac. Sci. Technol. B **10**, 336 (1993).
[11] S.S. Iyer, R.A. Metzger, and F.G. Allen, J. Appl. Phys. **52**, 5608 (1981).
[12] V.P. Kesan, S.S. Iyer, and J.M. Cotte, J. Cryst. Growth **111**, 847 (1991).
[13] K. Nakagawa and M. Miyao, J. Appl. Phys. **69**, 3058 (1991).
[14] R.A. Metzger and F.G. Allen, Surf. Sci. **137**, 397 (1984).
[15] F. Reif, *Fundamentals of Statistical and Thermal Physics*, Intern. Ed. (McGraw-Hill, New York, 1965).
[16] N.W. Ashcroft and N.D. Mermin, *Solid State Physics*, Intern. Ed. (Holt-Saunders, Tokyo, 1976).
[17] S. Fukatsu, K. Fujita, H. Yaguchi, Y. Shiraki, and R. Ito, Appl. Phys. Lett. **59**, 2103 (1991).
[18] S.A. Barnett and J.E. Greene, Surf. Sci. **151**, 67 (1985).
[19] H. Jorke and H. Kibbel, Thin Solid Films **183**, 323 (1989).
[20] H. Jorke, J.-H. Herzog, and H. Kibbel, Fresenius J. Anal. Chem. **341**, 176 (1991).
[21] K. Nakagawa, M. Miyao, and Y. Shiraki, Jpn. J. Appl. Phys. **27**, L2013 (1988).
[22] K. Nakagawa and M. Miyao, Thin Solid Films **183**, 315 (1989).
[23] D.J. Godbey and M.G. Ancona, Appl. Phys. Lett. **61**, 2217 (1992).
[24] S.A. Barnett, H.F. Winters, and J.E. Greene, Surf. Sci. **165**, 303 (1986).

[25] M.J. Aziz, J. Appl. Phys. **53**, 1158 (1982).
[26] M.J. Aziz, Appl. Phys. Lett. **43**, 552 (1983).
[27] J.Y. Tsao, *Materials Fundamentals of Molecular Beam Epitaxy* (Sandia National Laboratories, Albuquerque, NM, 1992).
[28] G.E. Becker and J.C. Bean, J. Appl. Phys. **48**, 3395 (1977).
[29] J.C. Bean, Appl. Phys. Lett. **33**, 654 (1978).
[30] J.F. Nützel, P. Brichzin, and G. Abstreiter, Appl. Surf. Sci. (to be published).
[31] H. Jorke and H. Kibbel, Appl. Phys. Lett. **57**, 1763 (1990).
[32] J.F. Nützel, M. Holzmann, P. Schittenhelm, and G. Abstreiter, Appl. Surf. Sci. (to be published).
[33] J. Wilhelm, W. Wegscheider, and G. Abstreiter, Surf. Sci. **267**, 90 (1992).
[34] W. Dondl, G. Lütjering, W. Wegscheider, J. Wilhelm, and R. Schorer, J. Cryst. Growth **127**, 440 (1993).
[35] K. Eberl, G. Krötz, R. Zachai, and G. Abstreiter, J. Phys. C **5**, 329 (1987).
[36] D.J. Godbey, J.V. Lill, J. Deppe, and K.D. Hobart, Appl. Phys. Lett. **65**, 711 (1994).
[37] D.J. Godbey and M.G. Ancona, J. Vac. Sci. Technol. B **11**, 1392 (1993).
[38] K. Muraki, S. Fukatsu, Y. Shiraki, and R. Ito, Appl. Phys. Lett. **61**, 557 (1992).
[39] F. Wu, S.G. Jaloviar, D.E. Savage, and M.G. Lagally, Phys. Rev. Lett. **71**, 4190 (1993).